Cubic Equations of State Applied to HT/HP and Highly Aromatic Fluids

K.S. Pedersen, SPE, Calsep A/S; **J. Milter,** SPE, Statoil; and **H. Sørensen,** SPE, Calsep A/S

Summary

Pressure/volume/temperature (PVT) data are presented for 38 reservoir fluids including fluids dominated by paraffins, heavy aromatic fluids with a significant content of C_{81+}, and high-temperature/high-pressure (HT/HP) reservoir fluids. By properly taking into account the compositional differences, these fluid types can all be represented using a classical cubic [Soave-Redlich-Kwong (SRK) or Peng-Robinson (PR)] equation of state (EOS) with volume correction. The plus fraction is split into carbon number fractions and EOS model parameters assigned to each fraction. To keep the number of components at a manageable level, the carbon number fractions are lumped into pseudocomponents, each containing several carbon number fractions. Hydrocarbons as heavy as C_{200} are considered when splitting up the plus fraction. Neglecting the content of components heavier than C_{80} will give a false picture of the phase behavior of heavy aromatic fluids. Correlations are presented for T_c, P_c, and ω as a function of molecular weight and density. Problems are experienced representing the thermal expansion of stable oils using a cubic EOS in the classical form. It is shown that this deficiency can be cured by introduction of a temperature-dependent volume correction term.

Introduction

Cubic EOS such as the SRK[1] and the PR[2] equations are widely used to simulate the phase behavior of gas and oil mixtures. The liquid densities predicted with these equations in the original form are generally too low, a deficiency that at least to some extent can be overcome by incorporating a volume shift parameter.[3] This is an additional EOS parameter affecting volumetric properties without influencing saturation points and phase compositions. To apply a cubic EOS with volume shift parameter, a critical temperature (T_c), a critical pressure (P_c), an acentric factor (ω), and a volume shift parameter (c) must be assigned to each component or pseudocomponent of the actual fluid.

A standard compositional analysis divides the components heavier than nC_6 into carbon number fractions.[4] Carbon number fraction C_N counts the hydrocarbons with a boiling point from that of $nC_{N-1}+0.5°C$ to that of $nC_N+0.5°C$. The C_7 fraction, for example, consists of the hydrocarbons with a boiling point between 69.3 and 98.9°C (0.5°C above the boiling point of nC_6 to 0.5°C above the boiling point of nC_7). Each carbon number fraction contains paraffinic (P) and naphthenic (N) as well as aromatic (A) components, each of which will have different T_c, P_c, and ω values and volume shift parameters. Despite these compositional differences, it is customary to use only one set of EOS parameters to represent a whole carbon number fraction. A compositional analysis usually ends with some plus fraction as with, for example, C_{10+}. The latter will contain C_{10} and heavier carbon number fractions. Using high temperature gas chromatography, it is possible to analyze to C_{80+}[5] or even to C_{100+}, but this type of analysis is not yet standard in the oil industry. There is generally a need for a simulated split-up of the plus fraction.

A generally valid characterization concept must be applicable to reservoir fluids of much varying PNA distribution. While par-

affins dominate among the C_{7+} components of most North Sea fluids, aromatic contents in excess of 50% are often seen in the C_{7+} fraction of reservoir fluids from the Middle East, China, and Venezuela.

Much exploration activity is currently directed toward deep reservoirs at HT/HP. The ability of the classical cubic EOS to represent the molecular interactions at such conditions has often been questioned. More sophisticated EOS have been proposed, some of which include terms to account for the strong repulsive forces acting at high pressures.[6–8]

Fluid Compositions and Experimental Data

PVT data have been investigated for a total of 48 fluid compositions. Fluids 1 through 38 are reservoir fluids, an overview of which is given in **Table 1.** These fluids can be divided into:
- 19 "ordinary" reservoir fluids (Fluids 1 through 19) comprising reservoir oils, gas condensates, and fluids that are near critical (NC) at reservoir conditions.
- 9 aromatic highly dense reservoir fluids (Fluids 20 through 28). The composition of one of these fluids is shown in **Table 2.**
- 10 HT/HP reservoir fluids.

The data material further includes thermal expansion data for 10 stable oils. Oil formation volume (or Bo) factors for these oils may be seen from **Table 3.** Because the data are for stable oils, the Bo factors are not influenced by gas liberation and thus provide a true picture of the thermal expansion.

Either differential depletion or constant mass expansion (CME) experiments have been conducted for the oil mixtures including the heavy oils in Table 1. The PVT data for the gas condensate mixtures, the NC fluids, and the HT/HP fluids comprise CME and constant volume depletion (CVD) data.

C_{7+} Characterization

Pedersen *et al.*[5] use the following distribution functions to split up the plus fraction

Molar: $\ln z_N = A + BC_N$ . . . . (1)

Density: $\rho_N = C + D \ln C_N$ . . . . (2)

Molecular weight: $M_N = 14 \, C_N - 4$. . . . . (3)

z_N = the mole fraction, ρ_N = the density, and M_N = the molecular weight of carbon number fraction C_N. The heaviest carbon number fraction considered by Pedersen *et al.* is C_{80}. The constants A, B, C, and D are found from the mass balance equations

$$z_+ = \sum_+^{C_{max}} z_i \text{ . . . . (4)}$$

$$M_+ = \frac{\sum_+^{C_{max}} z_i M_i}{\sum_+^{C_{max}} z_i} \text{ . . . . (5)}$$

$$\rho_+ = \frac{\sum_+^{C_{max}} z_i M_i}{\sum_+^{C_{max}} \dfrac{z_i M_i}{\rho_i}}, \text{ . . . . (6)}$$

where z_+, M_+, and ρ_+ are, respectively, the mole fraction, molecular weight, and the density of the plus fraction. To determine C and D, it is further required that the equation shall fit the density of the last defined carbon number fraction. With an analy-

TABLE 1—EXTRACT OF DATA AND SIMULATION RESULTS FOR THE 38 RESERVOIR FLUIDS CONSIDERED IN THE STUDY

Fluid No.	Fluid Type	P_{res} (bar)	T_{res} (°C)	P_{sat} (bar)	C_1 mol%	C_{10+} mol%	C_{10+} Density (kg/m^3)	C_{80+} mol%	P_{sat} SRK (bar)	% Dev.	P_{sat} PR (bar)	% Dev.	Z_{Exp} at P_{res}	$Z_{SRK-P(T)}$ at P_{res}	$Z_{PR-P(T)}$ at P_{res}
1	Oil	356	103.8	76.7	15.57	37.78	872	0.08	74.8	-2.5	75.1	-2.1			
2	Oil	(401)	97	108.5	23.71	34.06	880	0.22	101.1	-6.8	101.0	-6.9	2.320	2.256	2.282
3	Oil	—	99	130.8	27.64	27.37	875	0.09	121.3	-7.3	122.2	-6.6			
4	Oil	341	128	175.5	33.11	28.08	911	0.63	157.4	-10.3	156.4	-10.9			
5	Oil	301	84	190	39.24	54.89	936	0.32	167.9	-11.6	169.1	-11.0	2.154	2.261	2.159
6	Oil	268	92.8	267.9	45.34	27.98	887	0.05	243.9	-9.0	249.9	-6.7			
7	Oil	308.3	71.6	239	45.40	34.77	902	0.08	207.8	-13.1	210.8	-11.8			
8	Oil	464	112	244.5	47.83	17.10	844	0.02	232.5	-4.9	236.8	-3.1			
9	Oil	—	141	340.3	53.89	13.94	864	0.01	327.0	-3.9	334.1	-1.8			
10	Oil	281.6	100	61.5	17.81	50.18	899	0.55	68.0	+10.6	67.5	+9.8			
11	NC	436	150	321.5	54.13	8.17	858	0.01	334.4	+4.0	341.3	+6.2	1.291	1.284	1.296
12	Oil	—	165	368.0	57.41	10.43	857	0.00	362.3	-1.5	368.0	0.0			
13	Oil	—	125	404.8	59.15	21.36	873	0.05	384.2	-5.1	386.3	-4.6			
14	NC	403	142	390.6	62.36	8.98	858	0.01	403.6	+3.3	409.9	4.9	1.212	1.198	1.205
15	Cond	(644.3)	143	450.0	72.98	3.80	839	0.00	443.4	-1.5	444.6	-1.2	1.458	1.455	1.479
16	Cond	476	155	388.0	74.16	2.71	834	0.00	382.4	-1.4	389.7	+0.4	1.203	1.190	1.200
17	Cond	(598)	129	477.0	74.34	4.36	832	0.00	477.8	+0.2	480.6	+0.8	1.409	1.422	1.442
18	Cond	(401)	96.6	282.0	83.58	1.03	812	0.00	244.5	-13.3	252.0	-10.6	1.032	1.070	1.077
19	Cond	—	150.5	503.5	88.42	0.56	812	0.00	470.8	-6.5	451.2	-10.4	1.542	1.576	1.613
20	H Oil	231	55.0	202.6	38.78	57.23	956	0.00	172.4	-14.9	178.6	-11.8	1.730	1.728	1.731
21	H Oil	176	76.6	62	19.43	69.03	949	0.88	67.5	+8.9	67.1	+8.2			
22	H Oil	109.2	32.3	107.3	30.50	67.63	1005	1.22	100.9	-6.0	101.0	-5.9			
23	H Oil	(345.8)	41.2	129.3	34.71	63.99	980	0.24	126.6	-2.1	129.0	-0.2	3.558	3.550	3.564
24	H Oil	(176)	76.5	52.0	14.99	76.89	948	0.75	51.2	-1.5	50.9	-2.1	1.846	1.843	1.847
25	H Oil	—	76.6	62.0	20.05	69.92	948	0.77	67.1	+8.2	66.8	+7.7			
26	H Oil	(137.9)	48.9	45.9	18.92	76.34	1011	7.05	45.7	-0.4	44.9	-2.2	2.245	2.238	2.237
27	H Oil	(137.9)	48.9	44.1	18.58	78.74	1012	6.88	45.5	+3.2	44.7	+1.4	2.282	2.277	2.276
28	H Oil	(207.9)	48.9	63.1	25.61	71.29	1001	6.18	68.3	+8.2	67.1	+6.3	3.075	3.085	3.125
29	HT/HP	766.5	150	455.4	84.30	0.99	905	0.00	472.2	+3.7	491.9	+8.0	1.504	1.456	1.489
30	HT/HP	596	135	473.3	80.08	2.12	835	0.00	447.2	-5.5	457.1	-3.4	1.342	1.316	1.338
31	HT/HP	774.9	152	487.8	77.83	2.95	848	0.00	457.7	-6.2	468.1	-4.0	1.623	1.563	1.599
32	HT/HP	678	146	519.0	80.69	2.05	841	0.00	536.6	+3.4	512.1	-1.3	1.403	1.418	1.444
33	HT/HP	757	142	470.0	83.04	1.44	840	0.00	509.8	+8.5	494.1	+5.1	1.500	1.486	1.520
34	HTHT	681	147.5	576	80.98	2.10	842	0.00	541.0	-6.1	515.6	-10.5	1.425	1.413	1.440
35	HT/HP	794	150	394.6	80.54	1.28	829	0.00	368.1	-6.7	376.1	-4.7	1.532	1.498	1.535
36	HT/HP	775	152	480	78.23	2.66	838	0.00	454.2	-5.4	457.9	-4.6	1.591	1.564	1.602
37	HT/HP	791.3	100	775.7	92.01	1.77	835	0.00	777.1	+0.2	751.6	-3.1	1.617	1.602	1.637
38	HT/HP	911	167	397.8	71.07	4.83	842	0.00	405.6	+2.0	413.9	+4.0	1.777	1.830	1.881

Pressures in parentheses in the P_{res} column are not reservoir pressure but the pressure at which the reported Z factor (Z_{Exp}) was measured.

TABLE 2—MOLAR COMPOSITION OF HEAVY AROMATIC OIL (FLUID 22)			
Comp	Mol%	M	Density (kg/m³)
N_2	1.05		
CO2	0.06		
C_1	30.50		
C_2	0.03		
C_3	0.02		
iC_4	0.01		
nC_4	0.04		
iC_5	0.03		
nC_5	0.05		
C_6	0.33		
C_7	0.16	96	876
C_8	0.06	107	887
C_9	0.04	121	896
C_{10+}	67.62	451.3	1005

sis to, for example, C_{10+}, the constants C and D must fit the density of the C_9 fraction.

Different empirical correlations have been proposed in literature for estimating T_c, P_c, and ω of the C_{7+} fractions (Cavett,[9] Kesler and Lee,[10] and Pedersen et al.[5]). The correlations of Pedersen et al. take the form

$$T_c = c_1\rho + c_2 \ln M + c_3 M + \frac{c_4}{M} \dots \dots \dots (7)$$

$$\ln P_c = d_1 + d_2\rho^{d5} + \frac{d_3}{M} + \frac{d_4}{M^2} \dots \dots \dots (8)$$

$$m = e_1 + e_2 M + e_3 \rho + e_4 M^2, \dots \dots \dots (9)$$

where m = a function of the acentric factor

$$\text{SRK}: m = 0.480 + 1.574\omega - 0.176\omega^2 \dots \dots \dots (10)$$

$$\text{PR}: m = 0.37464 + 1.5422\omega - 0.26992\omega^2. \dots \dots \dots (11)$$

The correlations used for T_c, P_c, and ω are to be regarded as expressions capable of providing the mixture parameters a and b that will enable the EOS to match the phase behavior of reservoir fluids with a considerable C_{7+} content. The correlations are not to be regarded as expressions providing the real critical properties of heavy hydrocarbons. At least for components heavier than C_{20}, the critical point is an unattainable state.

The purpose of a cubic EOS is twofold. A primary purpose is to simulate phase boundaries and molar phase amounts. Secondly,

it is used to simulate phase densities. Introduction of a volume shift parameter as suggested by Peneloux and coworkers[3] permits these two goals to be dealt with separately. The molar volume with volume correction (V^{Peneloux}) and that without volume correction (V^{EOS}) are related as follows:

$$V^{\text{Peneloux}} = V^{\text{EOS}} - c, \dots \dots \dots (12)$$

where c = the volume shift or Peneloux parameter. The T_c, P_c, and ω correlations may therefore be developed to primarily provide correct phase boundaries and phase amounts. With that in place, the volume shift parameter can be used to correct for any deviations between the actual phase densities and those simulated with the EOS with no volume correction.

The Peneloux volume shift parameter of C_{7+} pseudocomponent i is found as

$$c_i = \frac{M_i}{\rho_i} - V_i^{\text{EOS}}. \dots \dots \dots (13)$$

M_i = the molecular weight, and ρ_i = the density of pseudocomponent i at 15°C and atmospheric pressure. V_i^{EOS} = the molar volume of pseudocomponent i at the same conditions using the appropriate EOS (SRK or PR) with no volume correction. Eq. 13 ensures that the Peneloux volume of pseudocomponent i agrees with the experimentally determined density at 15°C and atmospheric pressure.

Characterization to C_{200}

Pedersen et al.[5,11,12] have in previous publications ignored components heavier than C_{80}. To investigate the possible importance of components beyond C_{80}, the C_{81+} content was estimated by solving Eqs. 1 and 3 for each of the fluids in Table 1. The result may be seen from Table 1. All the heavy oils (Oils 20 through 28) except one (Oil 20) have a significant content of C_{81+}. In most of the remaining fluids, the content of C_{81+} is small or even negligible.

To accommodate for the C_{81+} content, the characterization procedure of Pedersen et al. was modified as follows:
• The heaviest hydrocarbon considered was increased from C_{80} to C_{200}.
• New coefficients were estimated in the correlations for T_c, P_c, and ω (Eqs. 7 through 9). The estimation was based on the PVT data for Fluids 1 through 28. Neither the HT/HP fluids (Fluids 29 through 38) nor the stable oils were considered in the estimation.

The limit of C_{200} is chosen to make sure all carbon number fractions present in significant amounts are accounted for. Splitting up the C_{10+} plus fraction of Fluid 22 (see Table 2), it was found that C_{200} was present in a mole % of 3.1×10^{-5}. In general, mole percentages below 10^{-4} will only marginally influence the phase behavior.

The resulting coefficients in Eqs. 7 through 9 are shown in **Table 4.** Separate coefficients were estimated for the SRK and PR equations. This has to do with different forms of the attractive

TABLE 3—EXPERIMENTAL AND SIMULATED BO FACTORS OF STABLE OILS						
Oil No.	T interval (°C)	Bo Exp.	Bo SRK-P	Bo PR-P	Bo SRK-P (T)	Bo PR-P(T)
39	84→15	1.061	1.027	1.022	1.045	1.045
40	83→15	1.056	1.027	1.022	1.045	1.045
41	82→15	1.050	1.026	1.022	1.044	1.044
42	81→15	1.049	1.027	1.022	1.043	1.043
43	86→15	1.054	1.033	1.027	1.048	1.043
44	83→15	1.054	1.034	1.028	1.048	1.048
45	99→15	1.081	1.047	1.039	1.069	1.068
46	106→15	1.080	1.043	1.036	1.068	1.068
47	83→15	1.067	1.035	1.029	1.053	1.052
48	98→15	1.075	1.041	1.034	1.065	1.064

TABLE 4—COEFFICIENTS IN EQS. 7 THROUGH 9 FOR USE WITH THE SRK AND PR EQUATIONS FOR T_c IN K AND P_c IN ATM

Coefficient	SRK	PR
c_1	3.04143×10^2	3.26725×10^2
c_2	4.84052×10	5.23447×10
c_3	7.10774×10^{-1}	5.77248×10^{-1}
c_4	3.80073×10^3	1.77498×10^3
d_1	3.05081	2.68058
d_2	-9.03352×10^{-1}	-5.32274×10^{-1}
d_3	2.33768×10^2	2.04507×10^2
d_4	-1.27154×10^4	-9.45434×10^3
d_5	0.25	0.25
e_1	4.96902×10^{-1}	1.89723×10^{-1}
e_2	5.58442×10^{-3}	7.42901×10^{-3}
e_3	1.01564×10^{-2}	3.28795×10^{-2}
e_4	-5.24300×10^{-6}	-7.36151×10^{-6}

terms in the two equations. For the same C_{7+} properties, the saturation point pressures simulated with the PR equation for fluids with a considerable content of C_{7+} will be 10 to 15% lower than with the SRK equation.

Eq. 9, with the coefficients in Table 4, will lead to low, often negative acentric factors for high molecular weight components. This may result in simulation of false liquid/liquid split. For carbon number fractions with a molecular weight greater than 1,000, the parameter m was therefore found from

$$m_i = \frac{1000 \times m_{M=1000}}{M_i}, \quad \dots\dots\dots\dots\dots\dots\dots\dots\dots\dots\dots (14)$$

where $m_{M=1000}$ = the value of m for a molecular weight of 1,000 and the density from Eq. 2. Still, the acentric factors of the heaviest hydrocarbon constituents may become fairly low. The acentric factor expresses the slope of the vapor pressure curve. For *n*-paraffins up to nC_{20}, the acentric factor is seen to increase with molecular weight, but there is no guarantee that this trend will continue for higher carbon number fractions. Secondly, the T_c, P_c, and ω correlations serve the purpose of generating mixture a and b parameters that will make the EOS match the phase behavior of the actual fluid. The absolute values of T_c, P_c, and ω do not count in themselves.

Nonzero binary interaction coefficients were used for binaries with a nonhydrocarbon component (N_2, CO_2, or H_2S),[13] while all hydrocarbon/hydrocarbon interaction parameters were set to zero. Positive binary interaction parameters will in general increase the saturation pressures (expand the two-phase region). As an alternative to using EOS-specific T_c, P_c, and ω correlations, one might use only one set of parameters and instead adjust the saturation points by introducing nonzero binary interaction coefficients. Positive binary interaction coefficients between hydrocarbons may, however, introduce false liquid/liquid split, as the interaction parameters will decrease the simulated attractive forces between the relevant component pairs. In general, it is more physically sound to modify the component properties to have the actual EOS represent the individual components correctly.

Thermal Expansion of Stable Oils

Table 3 shows experimental shrinkage factors for 10 stable oils in comparison with simulation results with the SRK-P and PR-P equations. It is seen that the thermal expansion is somewhat underpredicted. If the Peneloux parameters of the C_{7+} components as suggested by Eq. 13 are determined to match the liquid densities at 15°C and atmospheric pressure, too-high liquid densities will be simulated at higher temperatures. Although the errors on the SRK-P and PR-P Bo factors in Table 3 may not seem alarming, it is for a number of applications a serious problem if the thermal

expansion is systematically underestimated. Multiphase meters operating at elevated T and P can be mentioned as an example. The flow rates measured at meter conditions will usually have to be converted to standard conditions. Accurate flow rates at meter conditions are dependent on a correct description of the thermal expansion.

According to the ASTM 1250-80 correlation, the density, ρ, of a stable oil varies with temperature according to the formula (ρ in kg/m^3)

$$\rho_{T_1} = \rho_{T_0} e^{\{[-A(T_1-T_0)][1+0.8A(T_1-T_0)]\}} \dots\dots\dots\dots\dots\dots\dots (15)$$

T_0 = a reference temperature at which the density is known, and T_1 = the temperature for which the density is to be calculated. The constant A is found as

$$A = \frac{613.9723}{\rho_{T_0}^2}. \quad \dots\dots\dots\dots\dots\dots\dots\dots\dots\dots\dots\dots\dots\dots\dots (16)$$

This correlation is here used to introduce a temperature-dependent Peneloux parameter in the SRK-P and PR-P equations

$$c_i = c_{0i} + c_{1i}(T - 288.15). \quad \dots\dots\dots\dots\dots\dots\dots\dots\dots\dots\dots (17)$$

T = the absolute temperature in K, c_{0i} the usual Peneloux-parameter as determined from Eq. 13, and c_{1i} is a new temperature-dependent term determined to comply with the ASTM 1250-80 correlation. The last two columns in Table 3 show shrinkage factors for each of the 10 stable oils using temperature-dependent Peneloux parameters. The agreement is much improved as compared with the result of using a temperature-independent volume correction. **Fig. 1** shows measured molar volumes of Oil 42 at temperatures of 15 and 81°C in comparison with molar volumes simulated using the SRK equation with no volume correction, with a constant volume correction (SRK-P) and finally with a temperature-dependent volume correction [SRK-P(T)]. By comparing the experimental molar volumes with those simulated using the SRK equation, it is obvious that the volume correction needed depends on temperature. This is further illustrated by the SRK-P curve, which provides a match of the molar volume at 15°C, whereas the simulated molar volume at 81°C is too low. Using a temperature-dependent volume correction, the match of the experimental volumes is good at both temperatures.

Simulation Results

In the simulations, the C_{7+} fraction of each fluid was divided into 12 pseudocomponents. C_7, C_8, and C_9 were kept as separate fractions, while the heavier fractions were divided into a total of 9 pseudocomponents, each containing approximately the same weight amount.[11] No regression was performed to PVT data for the individual fluids. **Table 5** shows the heavy oil in Table 2 after being characterized for the SRK-P(T) equation.

Table 1 summarizes the simulation results for the reservoir fluids. The results comprise saturation points at reservoir temperature and, for most fluids, the Z factor at the reservoir pressure or
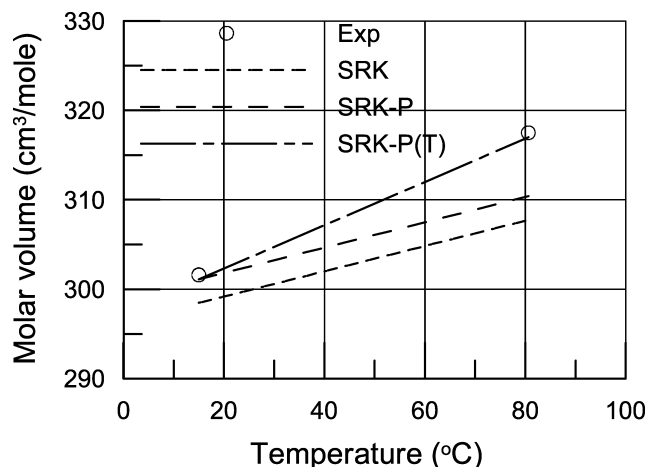

Fig. 1—Experimental and simulated molar volumes of Oil 42.

TABLE 5—THE HEAVY OIL IN TABLE 2 CHARACTERIZED FOR SRK-P (T)						
Comp	Mol%	T_c (°C)	P_c (bar)	ω	c_0 SRK	c_1 SRK
N_2	1.05	-146.95	33.94	0.040	0.92	0
CO_2	0.06	31.05	73.76	0.225	3.29	0
C_1	30.50	-82.55	46.00	0.008	0.63	0
C_2	0.03	32.25	48.84	0.098	2.63	0
C_3	0.02	96.65	42.46	0.152	5.06	0
iC_4	0.01	134.95	36.48	0.176	7.29	0
nC_4	0.04	152.05	38.00	0.193	7.86	0
iC_5	0.03	187.25	33.84	0.227	10.93	0
nC_5	0.05	196.45	33.74	0.251	12.18	0
C_6	0.33	234.25	29.69	0.296	17.98	0
C_7	0.16	326.02	26.66	0.337	74.99	0.08
C_8	0.06	339.57	26.12	0.386	70.08	0.07
C_9	0.04	355.19	25.03	0.447	66.91	0.05
C_{10}-C_{19}	16.27	455.88	18.19	0.876	73.57	-0.03
C_{20}-C_{24}	11.18	522.86	15.47	1.157	75.10	-0.09
C_{25}-C_{30}	10.10	583.55	13.98	1.369	72.56	-0.14
C_{31}-C_{36}	7.45	647.60	12.91	1.501	64.73	-0.19
C_{37}-C_{40}	5.25	697.37	12.31	1.511	55.51	-0.23
C_{41}-C_{46}	5.68	746.21	11.85	1.422	45.5	-0.26
C_{47}-C_{54}	4.80	812.95	11.37	1.174	30.06	-0.29
C_{55}-C_{67}	3.97	907.98	10.87	0.648	8.99	-0.32
C_{68}-C_{200}	2.92	1134.47	10.21	0.019	-26.84	-0.35

Note: c_0 is in cm^3/mol and c_1 in cm^3/(mol K).

another pressure above the saturation point. On the average, the saturation points found with the SRK equation are 2.3% too low, and those found with the PR equation are 2.1% too low. The Z factors above the saturation point found using SRK with temperature-dependent Peneloux correction [SRK-P(T)] are on the average 0.5% too low, and the PR-P(T) Z factors 0.9% too high.

The influence on the simulated saturation point at reservoir conditions of neglecting the C_{81+} content was tested for the 9 heavy oils. On the average, this made the saturation point increase by 10.6%.

For comparison, saturation points were simulated for Fluids 1 through 38 using the method of Pedersen *et al.*[5] A summary of the results may be seen in **Table 6.** For the "ordinary" oils, the results obtained with the method of Pedersen *et al.* are slightly better than with the method of the actual paper. For the heavy oils, the saturation points obtained with the method of Pedersen *et al.* are much too high. This is partly because of neglecting components heavier than C_{80}, and partly because of use of coefficients in Eqs. 7 through 9 that are inappropriate for oils of high density (highly aromatic oils). For the HT/HP fluids, the new correlations are slightly superior to those of Pedersen *et al.*

Fig. 2 shows experimental and simulated differential liberation GORs of Fluid 9. Liquid density results for the same experiment may be seen in **Fig. 3.**

Fig. 4 shows the CME liquid dropout curve of fluid No. 14 and **Fig. 5** the development in gas-phase Z factor of the same fluid. The Z factors below the saturation point of 450 bar are from a CVD experiment.

Fig. 6 shows experimental and simulated differential liberation GORs for Fluid 22. Liquid density results for the same experiment may be seen in **Fig. 7.** This fluid has a density above 950 kg/m³ at reservoir conditions, and the reservoir temperature is as low as 32.2°C.

Despite considerable variations in fluid type and reservoir conditions, the simulation results agree very well with the experimental observations. The small deviations seen could easily be eliminated by modifying the coefficients in Eqs. 7 through 9 to fit the PVT data for the individual compositions.

TABLE 6—AVERAGE DEVIATIONS BETWEEN SIMULATED (SRK EOS) AND MEASURED SATURATION POINTS				
Reservoir Fluid Type	Pedersen *et al.*		Method of Actual Paper	
	%BIAS	%ABS	%BIAS	%ABS
Ordinary	+0.8	4.9	-4.2	6.1
Heavy oils	+67.5	67.5	+0.4	5.3
HT/HP	+3.8	8.3	-1.2	4.8

Fig. 2—Experimental and simulated differential liberation GOR for Fluid 9 at 141°C.
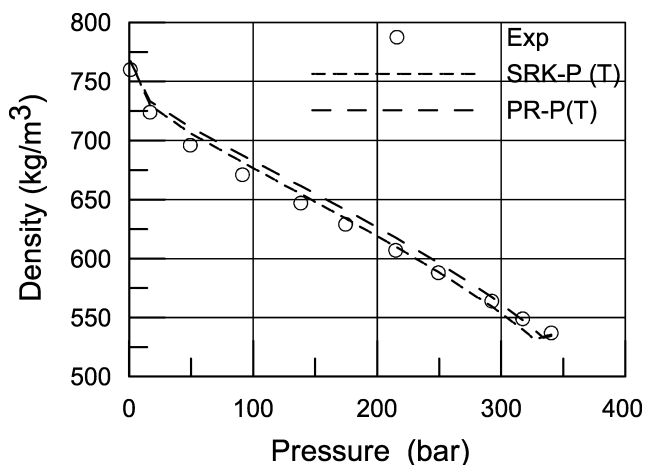
Fig. 3—Experimental and simulated differential liberation oil density for Fluid 9 at 141°C.
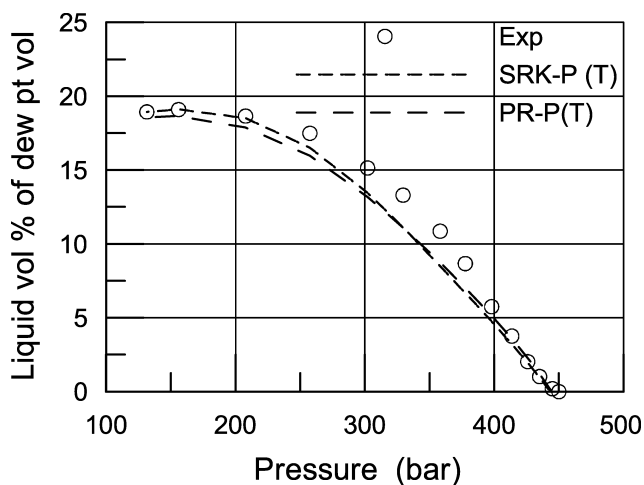

Fig. 4—Experimental and simulated CME liquid dropout for Fluid 15 at 143°C.
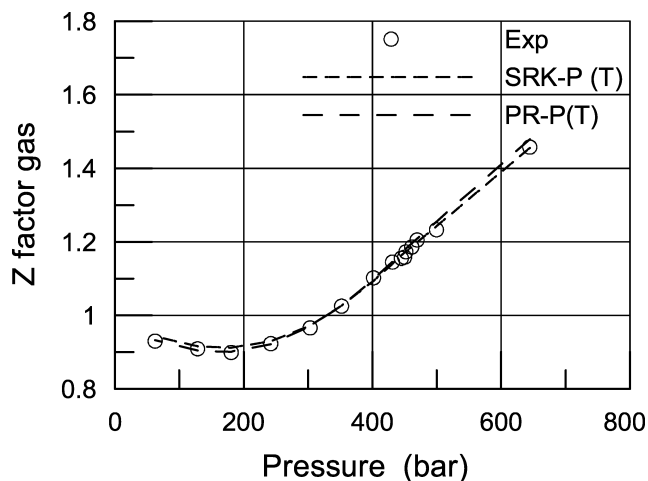

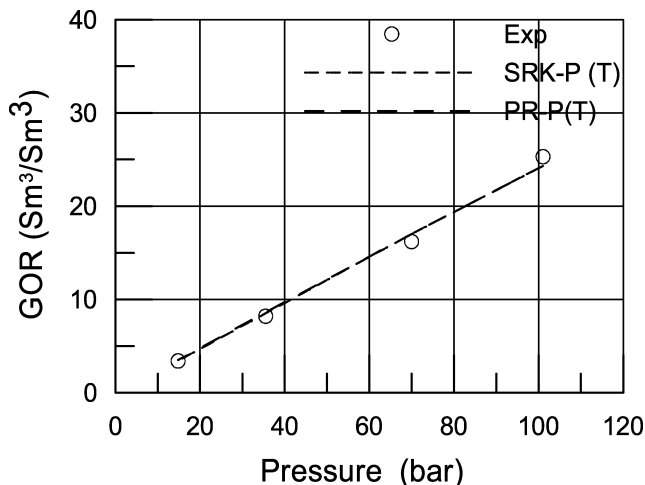Fig. 5—Experimental and simulated gas *Z* factors for Fluid 15 at 143°C.

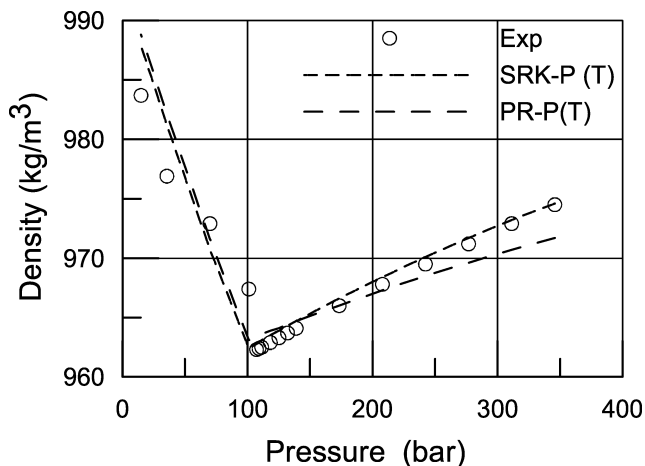Fig. 6—Experimental and simulated differential liberation GOR for Fluid 22 at 32.2°C.

Fig. 7—Experimental and simulated differential liberation oil densities for Fluid 22 at 32.2°C.

Fig. 8—Experimental and simulated CME liquid dropout for Fluid 36 at 152°C.

HT/HP Fluids

The new T_c, P_c, and ω correlations were tested out on the 10 HT/HP fluids (29 through 38) in Table 1. Simulation results of approximately the same quality were obtained, as for the fluids used to estimate new coefficients in the property correlations. Not only do the saturation points agree very well, but also the results

for the compressibility factors at high *T* and *P* give no support for the idea that more advanced EOSs should be needed to represent the fluid phase behavior at pressures of the order of 600 to 1000 bar and temperatures of the order of 150 to 180°C.
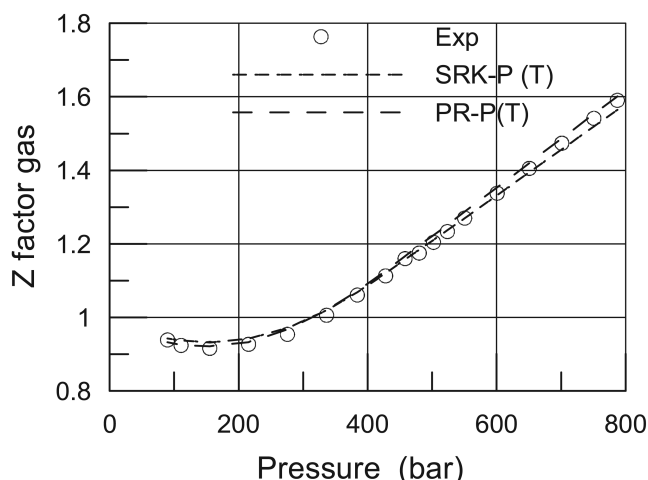
Fig. 9—Experimental and simulated gas *Z* factors for Fluid 36 at 152°C.

Fig. 8 shows the CME liquid dropout curve of Fluid 22 and **Fig. 9** the development in gas-phase Z factor of the same fluid. This fluid comes from a reservoir with a temperature of 152°C and a pressure of 775 bar. The Z factors below the saturation point of 480 bar are from a CVD experiment.

Conclusions

The phase behavior of "ordinary" reservoir fluids, heavy aromatic oils, as well as HT/HP reservoir fluids, can be well represented using the SRK or the PR equations with a temperature-dependent volume correction parameter. To properly represent the heavy end, the plus fraction must be split into carbon number fractions. Heavy aromatic reservoir fluids are significantly influenced by components heavier than C_{80}, for which type of fluids it is therefore recommended to consider components as heavy as C_{200} when splitting up the plus fraction. Correlations for T_c, P_c, and ω are presented that are applicable to a wide span of PNA distributions.

Nomenclature

A = constant defined in Eq. 1, aromatic or constant in ASTM 1250-80 correlation
B = constant defined in Eq. 1
c = volume shift (Peneloux) parameter
c_0 = temperature-independent Peneloux parameter
c_1 = temperature-dependent Peneloux parameter
c_1-c_4 = coefficients in T_c correlation (Eq. 7)
C = constant defined in Eq. 2 or carbon number
d_1-d_5 = coefficients in P_c correlation (Eq. 8)
D = constant defined in Eq. 2
e_1-e_4 = coefficients in correlation for m (Eq. 9)
Exp = experimental
M = molecular weight
N = number of components or naphthenic
P = pressure or paraffinic
PR-P = PR with Peneloux volume correction
PR-P(T) = PR with temperature-dependent Peneloux correction
SRK-P = SRK with Peneloux volume correction
SRK-P(T) = SRK with temperature-dependent Peneloux correction
T = temperature
z = mole fraction
%ABS = average absolute deviation
%BIAS = average percentage deviation
%Dev. = 100×(Exp-Simulated)/Exp
ω = acentric factor
ρ = density

Sub- and superscripts

EOS = equation of state with no volume correction
c = critical property
i = component index
N = carbon number fraction
max = heaviest hydrocarbon considered
0 = reference temperature
+ = plus fraction

Acknowledgment

The authors thank Statoil for permission to publish this paper.

References

1. Soave, G.: "Equilibrium Constants from Modified Redlich-Kwong Equation of State," *Chem. Eng. Sci.* (1972) **27,** 1197.
2. Peng, D.-Y. and Robinson, D.B.: "A New Two-Constant Equation of State," *Ind. Chem. Fundam.* (1976) **15,** 55.
3. Peneloux, A., Rauzy, E., and Fréze, R.: "A Consistent Correction for Redlich-Kwong-Soave Volumes," *Fluid Phase Equilibria* (1982) **8,** 7.
4. Katz, D.L. and Firoozabadi, A.: "Predicting Phase Behavior of Condensate/Crude-Oil Systems Using Methane Interaction Coefficients," *JPT* (November 1978) 1649.
5. Pedersen, K.S., Blilie, A.L., and Meisingset, K.K.: "PVT Calculations on Petroleum Reservoir Fluids Using Measured and Estimated Compositional Data for the Plus Fraction," *I&EC Research* (1992) **31,** 1378.
6. Benedict, M., Webb, G.R., and Rubin, L.C.: "An empirical equation for thermodynamic properties of light hydrocarbons and their mixtures. I. Methane, ethane, propane and butane," *J. Chem. Phys.* (1940) **8,** 334.
7. Donohue, M.D. and Vimalchand, P.: "The Perturbed-Hard-Chain Theory. Extensions and Applications," *Fluid Phase Equilibria* (1988) **40,** 185.
8. Lin, H.-M. *et al.:* "Cubic chain-of-rotators equation of state and VLE calculations," *Fluid Phase Equilibria* (1983) **13,** 143.
9. Cavett, R.H.: "Physical Data for Distillation Calculations—Vapor-Liquid Equilibria," *Proc.,* 1962 API Meeting, San Francisco, 351–366.
10. Kesler, M.G. and Lee, B.I.: "Improve the Predictions of Enthalpy of Fractions," *Hydrocarbon Processing* (1976) **55,** 153.
11. Pedersen, K.S., Thomassen, P., and Fredenslund, A.: "Thermodynamics of Petroleum Mixtures Containing Heavy Hydrocarbons. 1. Phase Envelope Calculations by Use of the Soave-Redlich-Kwong Equation of State," *Ind. Eng. Chem. Process Des. Dev.* (1984) **23,** 163.
12. Pedersen, K.S., Thomassen, P., and Fredenslund, A.: "Thermodynamics of Petroleum Mixtures Containing Heavy Hydrocarbons. 3. Efficient Flash Calculation Procedures Using the SRK Equation of State," *Ind. Eng. Chem. Process Des. Dev.* (1985) **24,** 948.
13. Pedersen, K.S., Milter, J., and Rasmussen, C.P.: "Mutual solubility of water and a reservoir fluid at high temperatures and pressures. Experimental and simulated data," *Fluid Phase Equilibria* (2001) **189,** 85.

SI Metric Conversion Factors

°F (°F − 32)/1.8		= °C
°F (°F + 459.67)/1.8		= °K
bar × 1.0*	E + 05	= Pa

* Conversion factor is exact.

Karen S. Pedersen is managing director of Calsep A/S, Denmark. e-mail: ksp@calsep.com. She is the author of more than 30 articles and a book on oil and gas properties. Pedersen holds an MSc degree in chemical engineering and a PhD degree in physical chemistry from the Technical U. of Denmark. **Jess Milter** is a staff engineer with Statoil Production Mamanger Statjord A, Norway. e-mail: jessmi@statoil.com. His research interests are within oil and gas production chemistry. Milter holds an MSc degree in chemical engineering from the Technical U. of Denmark and a PhD degree from the U. of Bergen in Norway. **Henrik Sørensen** is head of the software development team of Calsep A/S in Denmark. e-mail: hs@calsep.com. His research experience includes gas-water-salt phase equilibria applied to fluid inclusions. Sørensen holds a BSc degree in chemical engineering from the Technical U. of Denmark.